

Phase transitions in the ferroelectric crystals $[\text{CH}_3\text{NH}_3]_5\text{Bi}_2\text{Cl}_{11}$ and $[\text{CH}_3\text{NH}_3]_5\text{Bi}_2\text{Br}_{11}$ studied by the nonlinear dielectric effect

P. Szklarz,¹ M. Gałazka,² P. Zieliński,^{2,3} and G. Bator^{1,*}

¹*Faculty of Chemistry, University of Wrocław, Joliot-Curie 14, 50-383 Wrocław, Poland*

²*The H. Niewodniczański Institute of Nuclear Physics PAS, Radzikowskiego 152, PL-31-342 Kraków, Poland*

³*Cracow University of Technology, Institute of Physics, ul. Podchorążych 1, 30-084 Kraków, Poland*

(Received 23 February 2006; revised manuscript received 19 July 2006; published 13 November 2006)

The real part of the complex electric permittivity at low frequencies and at several biasing fields (between 0 and 5×10^5 V/m) has been measured in ferroelectric crystals $[\text{CH}_3\text{NH}_3]_5\text{Bi}_2\text{Cl}_{11}$ (MAPCB) and $[\text{CH}_3\text{NH}_3]_5\text{Bi}_2\text{Br}_{11}$ (MAPBB) in the temperature range covering the temperature of the ferroelectric phase transitions. Comparative measurements for the known triglycine sulphate $(\text{NH}_2\text{CH}_2\text{COOH})_3\text{H}_2\text{SO}_4$ crystal have been used as a test of the validity and of possible errors in the determination of the ferroelectric equation of state by the method applied. The estimates of the critical parameters T_C , γ , and δ then have been evaluated for MAPCB and MAPBB on the basis of the Widom-Griffiths scaling hypothesis. Complementary pyroelectric measurements of the spontaneous polarization providing the critical exponent β are in accordance with the parameters obtained.

DOI: [10.1103/PhysRevB.74.184111](https://doi.org/10.1103/PhysRevB.74.184111)

PACS number(s): 77.22.-d, 75.40.Gb, 72.20.Ht

I. INTRODUCTION

Measurement of the electric susceptibility in a biasing constant field is sometimes called nonlinear dielectric effect (NDE).^{1,2} It is a convenient method of studying ferroelectric phase transitions, especially those of second order. The application of the biasing electric field then allows one to scan the region of the critical point in a two-dimensional temperature-field space. Generally, the temperature dependence of the electric susceptibility measured in this way has the form of an asymmetric bell-like curve with a maximum which shifts towards higher temperatures with increasing biasing field. Far below and far above the phase transition region the curves tend to constant values corresponding to the low- and high-temperature limit susceptibilities, respectively. Consequently, such curves are concave—i.e., have negative second derivative close to the maximum—and convex—i.e., have positive second derivative in the low- and high-temperature limits. Thus, there are at least two points of vanishing second derivative on every such curve, one below (or to the left of) and one above (or to the right of) the maximum. The points are called inflection points. It has been shown by the present authors^{3,4} that for materials obeying the scaling-invariant equation of state there are in fact from one to three inflection points below the maximum depending on the values of the critical exponents β and γ . In particular there is always an inflection point exactly at the critical temperature for the classical (mean-field) exponents $\gamma=1$ and $\beta=\frac{1}{2}$.

What precedes the susceptibility is meant to be the static one. In practice, however, only ac data are available in most cases. Then, the low-frequency limit—i.e., that far below the normal dielectric absorption peak—of the real part of the complex electric susceptibility can be taken into account. Rigorously it is impossible to come too closely to the critical point because the dielectric absorption peak moves towards zero frequency when the critical point is approached. The effect is known as critical slowing down, which corresponds

to the relaxation time going to infinity. As a consequence, any experimental frequency becomes too large to be considered as the static limit. Moreover, the thermal conductivity tends to zero at the critical point so that the time needed to attain the thermal equilibrium after supplying a portion of heat to the system becomes infinite. Therefore, any experimental rate of changes of temperature is too rapid close enough to the critical point. No physical quantity measured in such conditions then corresponds to the thermal equilibrium. Related to the zero of thermal conductivity is also the phenomenon of passing from isothermal to adiabatic susceptibility.⁵

The use of a biasing field, which drives the system out of the critical point, allows one to evade all the described effects of the critical slowing down. Staying at a distance from the critical point in the temperature-field plane makes the dielectric absorption peak always lie at a finite frequency. Then, the low-frequency limit of the real susceptibility is, at least in principle, always possible to attain. The present paper deals with such a low-frequency electric susceptibility. We use the frequency independence of the real part of the susceptibility as a test of staying at the low-frequency limit because this corresponds to the practically vertical part of the Cole-Cole plot.⁶ As described in Sec. III and in Refs. 7–13 the analysis of the data obtained in the NDE allows one to determine, through so-called scaling invariants, all the parameters of the equation of state compatible with the scaling hypothesis. Such an analysis has been done for the known ferroelectrics TGS, TGSe, GPI, and DMAGaS.^{7,8,11}

In the present work the scaling equations of state are established for the $[\text{CH}_3\text{NH}_3]_5\text{Bi}_2\text{Cl}_{11}$ (MAPCB) and $[\text{CH}_3\text{NH}_3]_5\text{Bi}_2\text{Br}_{11}$ (MAPBB) crystals. These are relatively new materials belonging to the family of halogenoantimonates (III) and halogenobismuthates (III) (Ref. 14) or imidazolium tetrafluoroborate (Ref. 15). Particularly interesting are the recently synthesised methylammonium salts MAPCB (Ref. 16) and MAPBB (Ref. 17). Both of them show quasirigid anionic sublattices and orientationally disordered cat-

Phase diagram for MAPCB and MAPBB

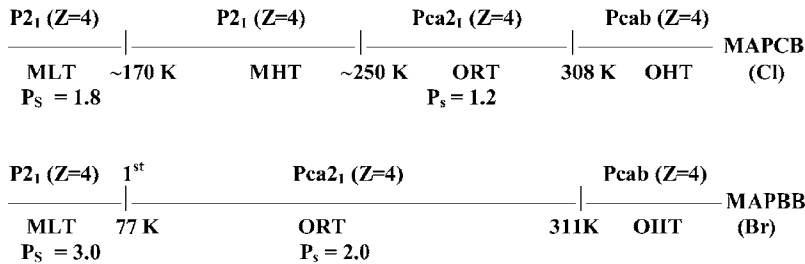


FIG. 1. Phase diagram for MAPCB and MAPBB

where : P_s - spontaneous polarization value [$10^{-2} \text{ C}\cdot\text{m}^{-2}$]
 OHT – orthorhombic system – high temperature phase
 ORT - orthorhombic system – room temperature phase
 MIIT – monoclinic system – high temperature phase
 MLT – monoclinic system – low temperature phase

ions undergoing a more or less definitive ordering at the paraelectric-ferroelectric phase transition. The anionic sublattice of both MAPCB and MAPBB is built of bioctahedral units ($\text{Bi}_2\text{Cl}_{11}^{5-}$). MAPCB is ferroelectric below 308 K,¹⁸ whereas MAPBB below 311 K.¹⁷ The transitions in both crystals are of the “order-disorder” type. In the crystal lattice of MAPCB (at room-temperature–ferroelectric-phase–orthorhombic, space group $Pca2_1$) three types of organic cations (CH_3NH_3^+) are found.¹⁹ The phase transition is related to the ordering of one type of the methylammonium cations, which are placed in centrosymmetric sites in the high-temperature phase. It is assumed that the same situation concerns the MAPBB crystal. In Fig. 1 we present the phase diagram for MAPCB and MAPBB with space groups of the particular phases.

Section II presents the details of experiments and Sec. III the rudiments of the analysis with the use of the scaling invariants. The equations of state are given in Sec. IV and verified with the pyroelectric data of the temperature dependence of the spontaneous polarization. The resulting equations of state involve critical exponents close but significantly different from the classical ones in some analogy to the existing data for the uniaxial ferroelectrics triglycine sulphate (TGS) and triglycine selenate (TGSe). They are also different from the universality classes following from the renormalization group theory. The physical reasons for that are discussed in Sec. V.

II. EXPERIMENTAL DETAILS

Crystals of $[\text{CH}_3\text{NH}_3]_5\text{Bi}_2\text{Cl}_{11}$ and $[\text{CH}_3\text{NH}_3]_5\text{Bi}_2\text{Br}_{11}$ were prepared as described earlier.¹⁷ The single crystals of MAPCB and MAPBB were cut perpendicular to the polar c axis. The dimensions of the sample were of order of $5 \times 3 \times 1 \text{ mm}^3$. The plates were silver painted. No anomaly on the frequency dependence of electric conductivity has been observed between 200 Hz and 1 MHz, indicating that effects of contacts in the dielectric response can be neglected. The thickness of the samples, d (usually close to 1 mm), was used for calculation of electric field intensity $E=U/d$, where U corresponds to voltage applied. The thickness of the

samples is given in corresponding captions of figures. The paraelectric-ferroelectric phase transition is related to the transformation from centrosymmetric to noncentrosymmetric group within orthorhombic system ($Pcab \rightarrow Pca2_1$). Single crystals of MAPCB and MAPBB are not monodomain, and ferroelectric domains structure appears below T_C . The crystals are not the proper ferroelastics in the vicinity of the ferroelectric phase transition; however, a spontaneous strain appears there as a secondary order parameter (see Sec. IV B).

The complex dielectric susceptibility $\chi^* = \chi' - i\chi''$ was measured with the Agilent 4284A Precision LCR meter at the frequency of 200 Hz and in the temperature range $T_C - 10 \text{ K} < T < T_C + 10 \text{ K}$, where T_C is a critical temperature of the ferroelectric crystal. The temperature was changed at a rate 0.02 K/min. We applied the external biasing field from the range between 0 and $5 \times 10^5 \text{ V/m}$. Between the LCR meter and a chamber with a sample the external dc voltage bias protection circuit was used as separation. The overall error in estimation of the real part of the complex electric susceptibility was about 5%.

The MAPCB and MAPBB crystals are usually small since they are difficult to grow. A polarizing microscope was used for preliminary selection of crystals free of visible growth defects. Another criterion of the choice of good crystals for the NDE measurements was the shape of the $\chi=f(T)$ dependence. Only those samples were chosen for which the maximum value of the static susceptibility at the zero biasing field was stronger than 2000 and 18 000 for MAPCB and MAPBB, respectively. One more criterion was the lack of inflection points right to the maximum at $E=0$, which are usually observed for imperfect crystals. Such additional inflection points are usually observed at zero-biasing field when a controlled amount of Bi atoms are substituted by Sb ones.²⁰ The NDE results obtained for the crystals selected as described above were reproducible from sample to sample, and the location of the maximum as well as inflection points at a given electric field was stable within 0.2 K.

The pyroelectric current was measured by a KEITHLEY 617 electrometer with temperature rate 0.5 K/min. Before measurements the single crystals were poled on cooling below the paraelectric-ferroelectric phase transition using voltage equal to 200 V and then short circuited for half an hour. Application of the larger voltage did not affect the spontane-

ous polarization value. Moreover, the use of negative voltage $-U$ resulted in reversal of the spontaneous polarization without changing its absolute value.

The dilatometric measurements were performed by a thermomechanical analyzer Perkin Elmer TMA-7 in the temperature range 140–300 K. The dimensions of the samples were of the order of $5 \times 3 \times 1$ mm³. The temperature scanning rate was equal to 4 K/min.

III. THEORY: ELECTRIC SUSCEPTIBILITY AT A NONZERO BIASING FIELD

The properties of a ferroelectric material can be described by an auxiliary thermodynamical potential (free energy) $F(P, E, T)$, where the polarization P is treated as a variable, whereas the temperature T and the field E as external parameters. The ferroelectric equation of state then is expressed by the condition $\frac{\partial F}{\partial P} = 0$ of the minimum of the free energy F with respect to the polarization P . While in Landau-type theories the free energy F is a polynomial in the variable P , the scaling hypothesis with nonclassical critical exponents implies the following nonanalytical form

$$F(P, E, T) = \frac{1}{2}C_2\tau P^2 + \frac{1}{\delta+1}C_{\delta+1}|P|^{\delta+1} - EP, \quad (1)$$

where

$$\tau = \text{sgn}(T - T_C)|T - T_C|^\gamma. \quad (2)$$

The corresponding equation of state then reads

$$E = C_2\tau P + C_{\delta+1}|P|^\delta \quad (3)$$

and is compatible with the Widom-Griffiths scaling hypothesis.^{21,22} The inverse of the isothermal equilibrium susceptibility,

$$\chi_T^{-1} = \left. \frac{\partial E}{\partial P} \right|_T = C_2\tau + \delta C_{\delta+1}|P|^{\delta-1}, \quad (4)$$

then is predicted to show critical behavior at $E=0$,

$$\chi_{T,E=0}^{-1} = \frac{\partial E}{\partial P} = \Gamma_\pm |T - T_C|^\gamma, \quad (5)$$

where the critical amplitudes are $\Gamma_+ = C_2$ for $T > T_C$ and $\Gamma_- = (\delta-1)C_2$ for $T < T_C$. Using Eqs. (3) and (4) one can deduce the temperature dependence of the static equilibrium susceptibility $\chi_{T,E}$ at a given value of the biasing field E . The actual shape of the corresponding curve depends crucially on the values of the critical exponents γ and δ . Generally, a maximum and a number of inflection points are expected³ on the temperature dependence of susceptibility $\chi_{T,E}$ at a given value of the biasing field E .

All the experiments also indicate an inflection point at a temperature T_{infl} inferior of the maximum at the position which is very weakly dependent on the biasing field. The explicit form of Eqs. (3) and (4) reveals, however, that in fact one deals here with a number of close inflection points and/or cusp singularities which merge into a single inflection point for certain particular values of the critical exponents δ and γ .³

It has been shown by Westwański and Fugiel²³ that some ratios independent of the electric field E and of the coefficients C_2 and $C_{\delta+1}$ can be built on the basis of the scaling hypothesis. These ratios are called scaling invariants. They correspond to the temperature of the maximum of the susceptibility or to the temperatures of the inflection points but with different biasing fields E . We have used the invariants to determine the critical exponents δ and γ in the equation of state. The scaling invariants used in the present work are the following. The invariant Q is defined in Ref. 23 as

$$Q = \frac{\chi(\tau_{\max}, E=0)}{\chi(\tau_{\max}, E \neq 0)}, \quad (6)$$

where $\tau_{\max} = T_{\max} - T_C$ corresponds to the reduced temperature at which the susceptibility exhibits maximum for the given value of the biasing field E . The invariant Q depends on the critical exponent δ only:^{7,24}

$$Q = \frac{\delta-1}{\delta-2}. \quad (7)$$

The invariant Γ is also independent of E , C_2 and $C_{\delta+1}$ are also invariant defined as³

$$\Gamma = \frac{\chi(\tau_{infl}, E=0)}{\chi(\tau_{infl}, E \neq 0)}, \quad (8)$$

where $\tau_{infl} = T_{infl} - T_C$ corresponds to the reduced temperature of an inflection point of the static susceptibility measured as a function of temperature at a biasing field E parallel to the ferroelectric axis. The explicit form of the invariant Γ for the equation of state given by Eq. (3) and for the unique inflection point right to the maximum (*iprm*) is

$$\Gamma = 1 - \delta + \frac{(\gamma+1)(\delta-1)^3}{\omega_{iprm}(\delta, \gamma)}, \quad (9)$$

where $\omega_{iprm}(\delta, \gamma)$ is a known but complicated function, which depends only on the critical exponents δ and γ . An explicit form of $\omega_{iprm}(\delta, \gamma)$ is given by Gałazka *et al.*³

In contrast to the previous invariants the following invariant Ω does not depend on the actual values of the susceptibility but only on the location of the maximum and of the inflection point with respect to the critical temperature:

$$\Omega = \frac{\tau_{\max}}{\tau_{infl}}. \quad (10)$$

The explicit formula for the invariant Ω is

$$\Omega = \left(\frac{(\gamma+1)(\delta-2)(\delta-1)^{(2/\delta)-1}}{\omega(\delta, \gamma)[\rho(\delta, \gamma)]^{-1/\delta}} \right)^{1/\gamma}, \quad (11)$$

where $\omega(\delta, \gamma)$ and $\rho(\delta, \gamma)$ are known functions given by Gałazka *et al.*³ Knowledge of T_C is not needed to determine the invariants Q and Γ but is necessary to establish the value of the invariant Ω from the experimental data.

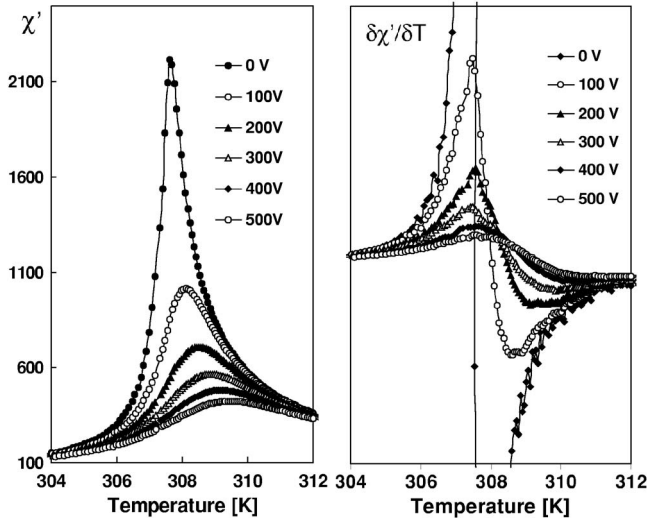


FIG. 2. The temperature dependence of susceptibility (left) and the temperature derivatives (right) of the susceptibility for MAPCB measured at a frequency of 200 Hz at different biasing voltages (thickness of the sample $d=0.75$ mm).

IV. RESULTS AND DISCUSSION

A. Determination of the critical parameters for MAPCB and MAPBB from an ac NDE experiment

The real part of the complex electric susceptibility is a good approximation of the static equilibrium susceptibility χ if the frequency is sufficiently low. A signature of the adequacy of this approximation is that the real part χ' does not depend on frequency in the range used in experiment. A frequency below 1 kHz is appropriate for most of ferroelectrics; however, for some crystals a dispersion of susceptibility is observed at even lower frequencies.²⁵ The dielectric absorption and dispersion for MAPCB and MAPBB are observed for frequencies higher than 1 MHz,^{26,27} so that the permittivity measured at the frequency (200 Hz) may be legitimately treated as static.

The temperature dependence of the real part of the complex susceptibility at several external electric field intensities and its temperature derivative for MAPCB and MAPBB is presented in Figs. 2 and 3. The electric field intensity was evaluated for each curve as $E=U/d$. A shift of the maximum of susceptibility with increasing biasing fields is well visible in figures. The main difference compared with TGS is that the absolute value of the permittivity is by a factor of 20 weaker. This makes the influence of the noises more pronounced. Of course the noises have more effect on the derivative curves. Nevertheless, each derivative curve shows clearly a maximum and a minimum. The maximum corresponds to the inflection point below the maximum of the susceptibility. One can easily see that the position of the maximum is indeed almost very weakly dependent on the biasing field that is witness to the proximity of the critical indices to the classical ones. The location of the minimum on the derivative curve indicates an inflection point to the right of the maximum (in what follows the subscript *iprm* will be dropped for brevity). As one can note, the temperature of this

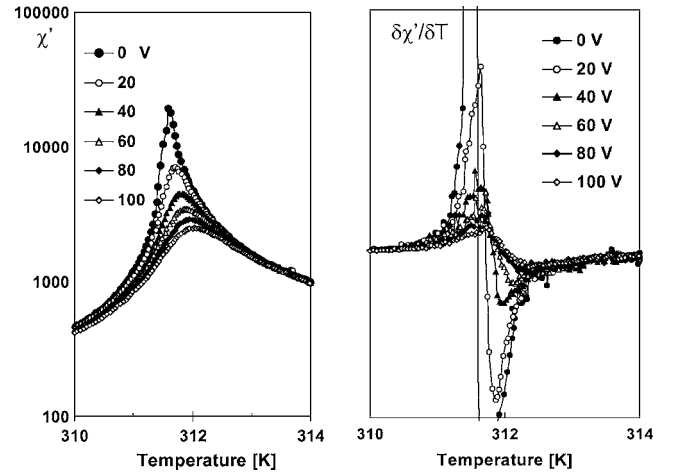


FIG. 3. The temperature dependence of susceptibility (left) and the temperature derivatives of the susceptibility (right) for MAPBB measured at a frequency of 200 Hz (thickness of the sample $d = 1.3$ mm).

inflection point clearly increases with increasing electric field E . In principle one could make use of the field dependence of the high-temperature inflection point to estimate directly the critical temperature and the critical exponents. We do not apply this method here as the one using the scaling invariants is more accurate. Nevertheless, it is interesting to know the errors arising with the present accuracy of the data. Thus, the relative error in the critical exponents δ and γ determined from the shift of the maximum is about 6%, whereas the absolute error in T_{iprm} amounts about 0.2 K.

Supposing that the measured electric susceptibility $\chi_{expt,E}$ is at most shifted by a constant value with respect to the static isothermal electric susceptibility χ_T of the material under discussion,⁵ we are entitled to assume that the power-law relation $T_{max}=T_C+\varphi_{max}E^{1/\Delta}$ is valid. The estimation of the critical index $1/\Delta$ has been done from the log-log plots given in Fig. 4. The power law is well verified, giving the values of $1/\Delta=0.76$ for MAPCB and for MAPBB $1/\Delta=0.72$. For the classical values of the critical exponents $\gamma=1$, $\delta=3$, the value of $1/\Delta=\frac{\delta-1}{\gamma\delta}$ equals 0.66. The estimated values of $1/\Delta$

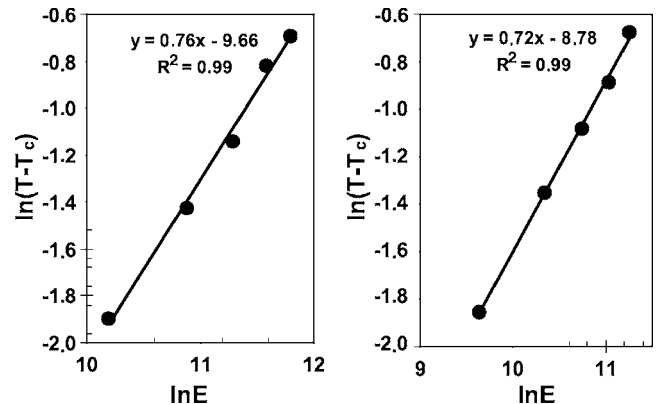


FIG. 4. Log-log plots of the reduced temperature of the maximum of the susceptibility, $T-T_C$, versus biasing field E giving an estimation of $1/\Delta$ for MAPCB (left figure) and MAPBB (right figure).

TABLE I. The critical parameters for TGS, MAPCB, and MAPBB.

	T_C [K]	γ	δ	$1/\Delta$	Q	Ω	Γ
TGS	322.21	0.998	3.14	0.67	1.709	0.585	1.182
MAPCB	307.65	0.985	3.47	0.76	1.680	0.584	1.142
MAPBB	311.52	0.989	3.40	0.72	1.711	0.564	1.167

may indicate a nonclassical behavior of the crystals studied.

We have estimated the values of the critical exponents γ and δ on the basis of a numerical analysis of the invariants Q , Γ , and Ω . As a reference system to test the method and estimate possible errors we have selected triglycine sulphate (TGS) crystals. This is a well-known uniaxial ferroelectric thoroughly investigated by numerous authors.⁷ The results (see Table I) indicated that the exponents obtained with the methods applied in this paper were reliable.

Figure 5 shows the dependence of the invariant Q , Γ , and Ω on the electric field value for MAPBB. Within the limits of experimental error, the value of the invariants Q , Γ and Ω , are constant and independent of the field E . The experimental values of these invariants have been obtained as the mean value for all the fields used. The estimated values of γ and δ are collected in Table I. Their nonclassical values indicate in our opinion the nonclassical behavior of the crystals studied. Calculated values of $1/\Delta$ using the estimated values of γ and δ are equal to 0.76 and 0.72 for MAPCB and MAPBB, respectively, and are with acceptable errors consistent with those obtained from the shift of the maximum with the biasing field.

B. Spontaneous polarization measurements

In order to verify the validity of the critical exponents obtained in the ac NDE we have performed measurement of the spontaneous polarization for the MAPCB and MAPBB crystals and fit the parameters to the experimental data. The experiment was carried out in the following way. First the samples were poled while cooling from above the paraelectric-ferroelectric phase transition temperature; the dc electric field was equal to +200 kV/m. The pyroelectric cur-

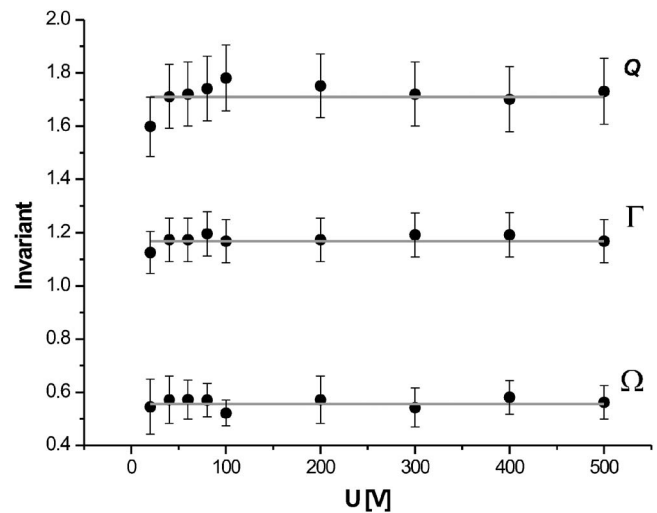


FIG. 5. Values of invariant and mean values Q , Γ , and Ω versus voltage for MAPBB.

rent I_{pyro} was then measured on heating of the crystal. The spontaneous polarization ΔP_S was calculated from the following equation:

$$\Delta P_S = \frac{\int I_{pyro} dt}{S}, \quad (12)$$

where S is the area of the sample. The polarization in the paraelectric phase was assumed to be zero. The spontaneous polarization P_S as a function of temperature for MAPCB and MAPBB is shown in Fig. 6. The P_S values are equal to about 0.7×10^{-2} C/m² at 297 K and 2.7×10^{-2} C/m² at 286 K for MAPCB and MAPBB, respectively. The solid line corresponds to the fit calculated for the parameters of the equation of state [Eq. (3)], C_2 , $C_{\delta+1}$, and β . The well-known Widom equality $\gamma = \beta(\delta - 1)$ resulting from the scaling equation of state allows us to compare the values of β with those obtained on the basis of the invariants analysis. As a matter of fact only the ratio $C_{\delta+1}/C_2$ may be estimated in this way. This ratio is equal to 3.85 and 3.91 for MAPCB and MAPBB, respectively. The estimated values of the critical exponents for MAPCB $\beta = 0.401$ and for MAPBB $\beta = 0.408$ are in good accordance with those obtained on the basis of

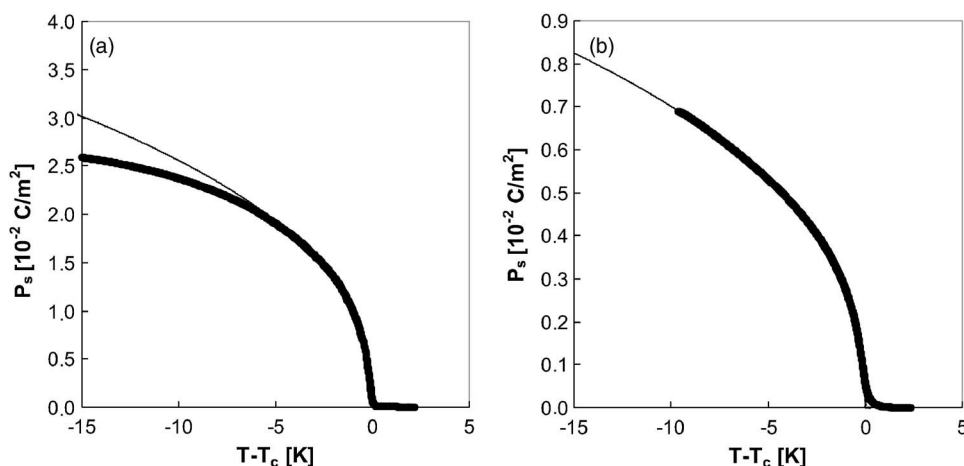


FIG. 6. The spontaneous polarization P_S as a function of temperature (a) for MAPBB and (b) for MAPCB at the heating rate 1 K/min.

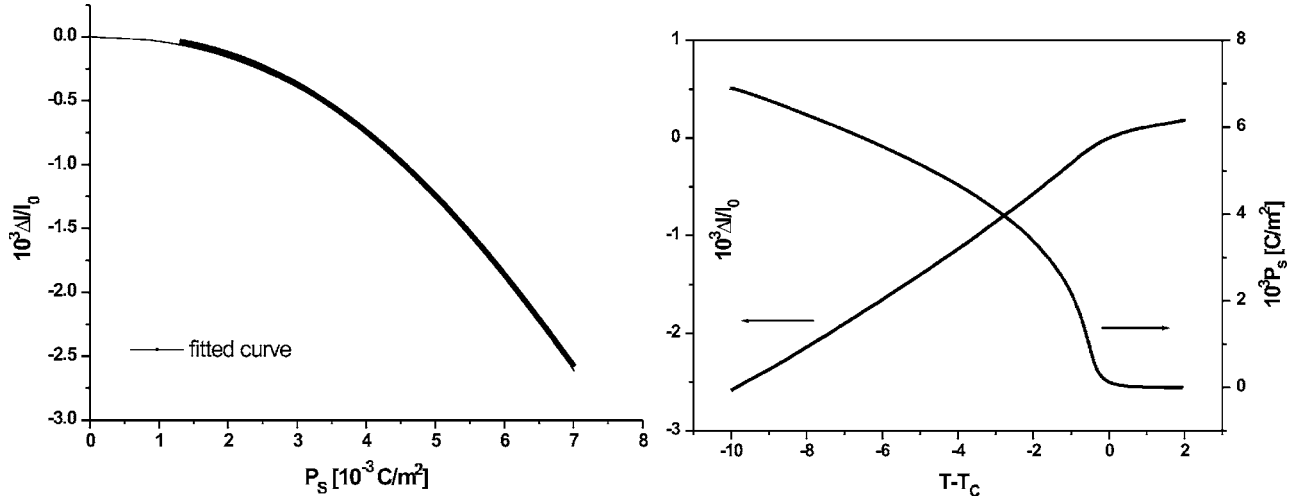


FIG. 7. Temperature dependence of the spontaneous polarization P_S and linear dilation $\Delta l/l$ along the polar axis in MAPCB (right). The dependence of $\Delta l/l$ versus P_S and the curve fitted to the power law $\varepsilon = -\frac{f}{c}|P|^{(\delta+1)/2}$ (left).

the invariants analysis (0.399 for MAPCB and 0.412 for MAPBB). However, it should be noted that for MAPBB the shape of the spontaneous polarization curve is well reproduced by theory only in the temperature range close to T_C for $T-T_C > -5$ K. Attempts to fit the critical parameters in a wider temperature range give unreasonable values. It is interesting that for MAPCB the shape of the curve of the temperature dependence of P_S is correctly reproduced by this theory in a wider temperature range.

The ferroelectric phase transition in MAPCB and MAPBB is accompanied by a deformation of the crystal (improper ferroelastic). The corresponding strain coupled with the order parameter involves a shortening in the direction of the polar axis and a dilatation in the other directions so that the total volume is not affected. This “pancake” strain, denoted here by ε , increases with increasing polarization, as being a secondary order parameter. The volume change, which amounts to the thermal expansion, does not show any anomaly at the phase transition. In order to take into account the pancake strain two new terms should be added to the free energy represented by Eq. (1):

$$F_\varepsilon = \frac{1}{2}c\varepsilon^2 + f\varepsilon|P|^{(\delta+1)/2}, \quad (13)$$

where c is an elastic constant and f a coupling coefficient. The condition of minimum with respect to ε requires that

$$\varepsilon = -\frac{f}{c}|P|^{(\delta+1)/2}, \quad (14)$$

which equality, when inserted into the new terms, brings the total free energy to the form of Eq. (13),

$$F_\varepsilon = \frac{1}{2}C_2\tau P^2 + \frac{1}{\delta+1}\tilde{C}_{\delta+1}|P|^{\delta+1}, \quad (15)$$

with only the coefficient $C_{\delta+1}$ renormalized:

$$\tilde{C}_{\delta+1} = C_{\delta+1} - \frac{\delta+1}{2} \frac{f^2}{c}. \quad (16)$$

The free energy, Eq. (1), then corresponds to a stressed crystal, where no strain is allowed, whereas Eq. (15) describes a nonloaded crystal. It is clear that the critical exponents are equal in both cases. To verify the validity of the theory Eq. (14) should be checked experimentally. Figure 7 presents the temperature dependence of the relative shortening of the polar axis—i.e., a quantity proportional to the pancake strain ε . A base line corresponding to a trend independent of the phase transformation has been subtracted. A power law then has been fitted to the dependence of the strain ε on the reduced temperature τ : $\varepsilon \propto \tau^A$. The fitted value of the exponent $A=2.22$ agrees very well with the $(\delta+1)/2=2.24$, which is witness to the consistency of our results with the scaling equation of state.

V. CONCLUSIONS

Nonclassical and nonuniversal critical exponents β , γ , and δ satisfying the scaling relation are found for the uniaxial ferroelectrics MAPBB and MAPCB on the basis of the low-frequency electric susceptibility measured in a constant biasing electric field (see Table I). Scaling invariants have been used to analyze the data. The values of the invariants have turned out to be constant within experimental error as is required by the scaling hypothesis. To test the quality of our data and the adequacy of our theoretical analysis we have applied the same procedures to the known ferroelectric triglycine sulfate $(\text{NH}_2\text{CH}_2\text{COOH})_3\text{H}_2\text{SO}_4$, TGS, and have obtained the results consistent with the values published earlier.^{7,24} Thus, the alkylammonium salts MAPCB and MAPBB fall into the same category as TGS and TGSe where the scaling equation of state [Eq. (3)] gives a more satisfactory description than the classical Landau theory. A common feature of these materials is that the critical exponents involved in the equation of state are neither classical nor corresponding to a universality class known from the renormal-

ization group theory. A large temperature range in which our description is adequate indicates that our results do not concern the closest vicinity of the critical point as required by the Ginzburg criterion. Therefore, we deal here with phenomena different or occurring in addition to the critical behavior. A crossover or even a series of crossovers resulting in some effective critical exponents²⁸ seems to be the most plausible explanation of our observations. A microscopic theory explaining the values obtained for the given materials in the well-defined experiment is still to be done. The critical exponent δ obtained in this work for the MAPCB crystal provides the ratio of the Curie constants $C_-/C_+=2.47$ which is still too low in comparison with experimental value [3.85

(Ref. 16)] obtained for this material at the zero-bias field. We have just constructed an equation of state also compatible with the scaling hypothesis but different from Eq. (3). This equation can make the ratio of the Curie constants dependent on some other parameters than only the critical exponents. Work is in progress to check the validity of this equation of state for the ensemble of data for the materials under study.

ACKNOWLEDGMENT

This work was supported by the Polish State Committee for Scientific Research (Project No. 3 T09A 023 26).

*Electronic address: gb@wchuwr.chem.uni.wroc.pl

- ¹S. Kielich, in *Dielectric and Related Molecular Processes*, edited by M. Davies (The Chemical Society, London, 1972).
- ²A. H. Piekara, *Eur. J. Phys.* **2**, 10 (1981).
- ³M. Gałązka, P. Szklarz, G. Bator, and P. Zieliński, *J. Phys.: Condens. Matter* **18**, 7145 (2006).
- ⁴M. Gałązka, P. Szklarz, G. Bator, and P. Zieliński, *Solid State Phenom.* **112**, 141 (2006).
- ⁵J. Bornarel and V. H. Schmidt, *J. Phys. C* **14**, 2017 (1981).
- ⁶K. S. Cole and R. H. Cole, *J. Chem. Phys.* **9**, 341 (1941).
- ⁷M. Mierzwa, B. Fugiel, and K. Ćwikiel, *J. Phys.: Condens. Matter* **10**, 8881 (1998).
- ⁸B. Fugiel, M. Pardała, J. Pawlik, and G. Sowa, *Phys. Lett. A* **209**, 373 (1995).
- ⁹W. S. M. Fally, W. Schranz, and D. Havlik, *Phys. Rev. B* **53**, 14769 (1996).
- ¹⁰F. Jona and G. Shirane, *Phys. Rev.* **117**, 139 (1960).
- ¹¹B. Fugiel, *Physica B* **325**, 256 (2003).
- ¹²J. Baran, G. Bator, R. Jakubas, and M. Śledź, *J. Phys.: Condens. Matter* **8**, 10647 (1996).
- ¹³R. Tchukvinskyi, R. Cach, and Z. Czaplá, *Z. Naturforsch., A: Phys. Sci.* **53**, 105 (1998).
- ¹⁴L. Sobczyk, R. Jakubas, and J. Zaleski, *Pol. J. Chem.* **71**, 265 (1997).

- ¹⁵Z. Pająk, P. Czarnecki, B. Szafrńska, H. Maluszynska, and Z. Fojud, *Phys. Rev. B* **69**, 132102 (2004).
- ¹⁶R. Jakubas, L. Sobczyk, and J. Lefebvre, *Ferroelectrics* **100**, 143 (1989).
- ¹⁷R. Jakubas, *Solid State Commun.* **69**, 267 (1989).
- ¹⁸P. Carpentier, J. Lefebvre, and R. Jakubas, *Acta Crystallogr., Sect. B: Struct. Sci.* **51**, 167 (1995).
- ¹⁹I. Belkhal, R. Mokhlisse, B. Tanouti, N. B. Chanh, and M. Couzi, *J. Alloys Compd.* **188**, 186 (1992).
- ²⁰M. Wojtaś, G. Bator, R. Jakubas, and J. Zaleski, *J. Phys.: Condens. Matter* **13**, 8831 (2001).
- ²¹B. Widom, *J. Chem. Phys.* **43**, 3898 (1965).
- ²²R. B. Griffiths, *Phys. Rev.* **158**, 176 (1967).
- ²³B. Westwański and B. Fugiel, *Phys. Rev. B* **43**, 3637 (1991).
- ²⁴A. Otolińska and B. Westwański, *J. Phys.: Condens. Matter* **12**, 1473 (2000).
- ²⁵G. Bator and R. Jakubas, *J. Phys. Soc. Jpn.* **72**, 2369 (2003).
- ²⁶C. Pawlaczyk, R. Jakubas, K. Planta, C. Bruch, and H.-G. Unruh, *J. Phys.: Condens. Matter* **4**, 2695 (1992).
- ²⁷C. Pawlaczyk, K. Planta, C. Bruch, J. Stephan, and H.-G. Unruh, *J. Phys.: Condens. Matter* **4**, 2687 (1992).
- ²⁸K. Binder, G. Meissner, and H. Mais, *Phys. Rev. B* **13**, 4890 (1976).